Elements of image processing in localization microscopy

2013 J. Opt. 15 094012

(http://iopscience.iop.org/2040-8986/15/9/094012)

IOP PUBLISHING JOURNAL OF OPTICS
J. Opt. **15** (2013) 094012 (7pp) doi:10.1088/2040-8978/15/9/094012

Elements of image processing in localization microscopy

Eric J Rees[1], Miklos Erdelyi[1], Gabriele S Kaminski Schierle[1], Alex Knight[2] and Clemens F Kaminski[1]

[1] Department of Chemical Engineering and Biotechnology, University of Cambridge, Pembroke Street, Cambridge, CB2 3RA, UK
[2] Analytical Science Division, National Physical Laboratory, Hampton Road, Teddington, TW11 0LW, UK

E-mail: ejr36@cam.ac.uk and cfk23@cam.ac.uk

Received 11 February 2013, accepted for publication 12 April 2013
Published 10 September 2013
Online at stacks.iop.org/JOpt/15/094012

Abstract
Localization microscopy software generally contains three elements: a localization algorithm to determine fluorophore positions on a specimen, a quality control method to exclude imprecise localizations, and a visualization technique to reconstruct an image of the specimen. Such algorithms may be designed for either sparse or partially overlapping (dense) fluorescence image data, and making a suitable choice of software depends on whether an experiment calls for simplicity and resolution (favouring sparse methods), or for rapid data acquisition and time resolution (requiring dense methods). We discuss the factors involved in this choice. We provide a full set of MATLAB routines as a guide to localization image processing, and demonstrate the usefulness of image simulations as a guide to the potential artefacts that can arise when processing over-dense experimental fluorescence images with a sparse localization algorithm.

Keywords: localization microscopy, super-resolution, image processing, software

S Online supplementary data available from stacks.iop.org/JOpt/15/094012/mmedia

(Some figures may appear in colour only in the online journal)

1. Introduction

Many of the most striking observations in recent biological research have been made possible by super-resolution microscopy techniques. These techniques can image fluorescently labelled biological structures with near to electron microscope resolution; and as light-based methods they are compatible with physiological (i.e. wet) conditions. Localization microscopy is one of the most important types of super-resolution imaging: it is the class of methods including PALM, (*d*)STORM, and GSDIM which are based on the precise determination of fluorophore positions on a specimen, followed by computational reconstruction of a super-resolved image [1–4]. These techniques are ideally suited to determining the morphology of small intracellular structures such as the actin cytoskeleton and other filamentous assemblies like the highly packaged von Willebrand Factor stored within Weibel–Palade bodies [5], as well as protein aggregates like beta Amyloid fibrils associated with Alzheimer's disease [6].

A general outline of localization microscopy is as follows. A specimen is labelled using photoswitchable fluorophores. Using a conventional fluorescence microscope and correct conditions (laser intensity, label density, buffer solution, camera integration time) a series of images of the specimen can be captured which contain a 'blinking' fluorescence signal. In these images, sparse or sometimes partially overlapping spots of fluorescence are obtained from random subsets of the fluorophores on the specimen. These results are processed computationally, as illustrated in figure 1. In a simple 'sparse' localization algorithm, the position of each fluorophore is inferred as corresponding to the centre position of each spot of fluorescence, and experimentally this can be determined by computational fitting as precisely as 10–20 nm. Once the positions of

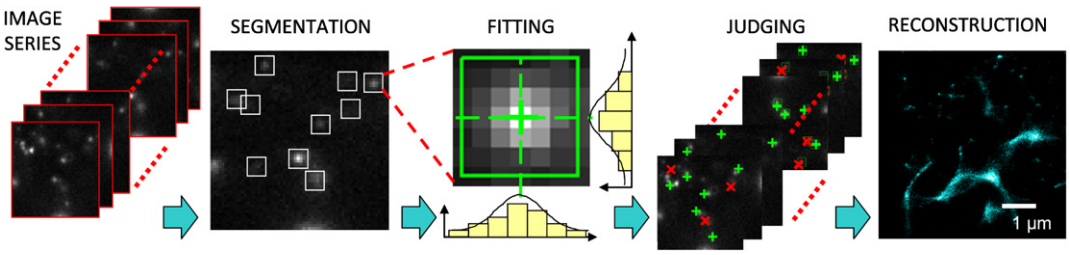

Figure 1. Image processing in localization microscopy. Spatially sparse fluorescence images are typically processed by a 'segmentation and Gaussian fitting' algorithm, which identifies bright spots that potentially correspond to fluorophores and then determines the precise position of each candidate by fitting a 2D Gaussian to the fluorescence signal. Candidates that are too dim, or imprecisely determined, are rejected by a judging method. Precise, robust localizations are used to reconstruct the super-resolution image of the specimen by plotting the density of localizations.

many fluorophores on the specimen have been determined, the specimen can be visualized with high resolution using a computational image reconstruction method, which visualizes the localized fluorophore density [7, 8].

Overall, the difference between a conventional fluorescence and a localization microscope is that the former senses the presence of a fluorophore by imaging a spread of photons on a camera, while the latter determines the fluorophore position as a localization—via an additional, computational step that follows on from capturing the conventional image data. Whereas a traditional fluorescence image of a single molecule might comprise a few thousand photons distributed over a diffraction-limited and relatively large point spread function (PSF), the same measurement could be interpreted as a single localization, with a much more tightly defined position that corresponds to the centre position of the N photons. Because the localization is determined with a narrower response function, by a factor of about $N^{-1/2}$, it supports a finer resolution.

A fundamental aspect of localization microscopy is that, in addition to the optical microscope itself, a major element of the imaging system is software—for position inference and subsequent reconstruction of the super-resolved image. The role of software is simple to describe; however there are many distinct implementations. In particular there are choices related to background subtraction and fitting algorithms [9–13], quality control (rejection of false-positive localizations) and image reconstruction technique [7, 8]. This complexity has two consequences for experimentalists. First, it means they need to be aware of the several issues that can affect the quality of their super-resolved images. Second, it raises the need for a general mathematical description that is applicable to various implementations, so that experiments can be treated as well-defined measurements and compared on a sound basis. We have recently worked on such a description [14], in order to study the resolution of localization microscopy images. Our model describes localization microscopy as (in mathematical terms) two steps: firstly localization of fluorophore positions, and secondly visualization of the structure based on these positions. The resolution of final reconstructed image is found to be limited by the finite error that affects localizations in step 1, and also by the finite amount of smoothing that must be applied to visualize them in step 2. In practice, localization microscopy software includes a third function as well as these two steps: it also includes quality control methods which aim to exclude spurious or imprecise localizations, without excluding true ones—the limitations of these quality control steps when dealing with real experimental data and different localization algorithms (e.g. for dense fluorescence data) are an interesting area of current research.

In this paper we summarize the elements of image processing in localization microscopy, as a complement for experimental guides such as [15–17]. A key issue for software is the localization bias that mars the fidelity of super-resolved images when algorithms are applied to denser fluorescence signals than they are able to address. We demonstrate this important issue with simulated and experimental data and a sparse algorithm; and we make available our set of MATLAB scripts for image simulation, localization, visualization and post-processing.

2. Methods

2.1. Image simulation

Simulated localization microscopy image data were prepared as follows, based on an established method [18]. For a single fluorophore simulation, the position of the fluorophore is translated onto a simulated EMCCD grid. Using a Gaussian approximation for the point spread function (PSF), the proportion of the PSF that falls into each pixel on the EMCCD is integrated and the expected number of photons collected in each pixel is established by allocating this proportion of its photon yield (many typical experimental yields are tabulated [19]). Because photon arrival is a stochastic process, this expected number of photons must then be replaced, independently for each pixel, by a random number drawn from a Poisson distribution with a mean equal to the expected photon number. Finally, random camera readout noise, typically drawn from a Gaussian distribution, is added to each camera pixel. In the case of a multi-fluorophore specimens, a random subset of fluorophores are chosen to be 'active' in each frame and their images are summed as for the single fluorophore simulation, before finally adding camera noise.

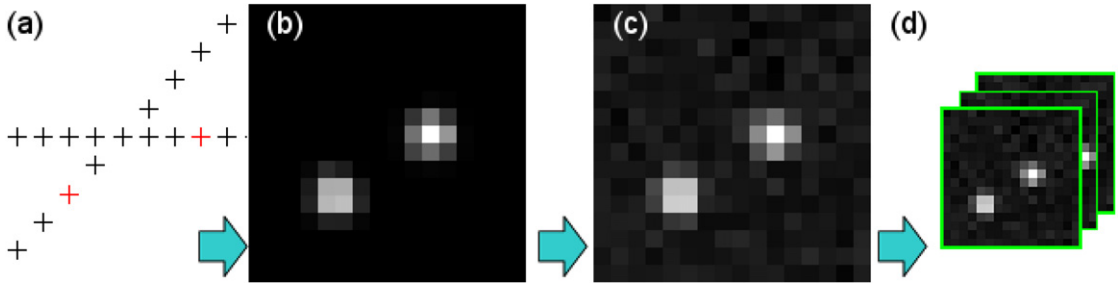

Figure 2. Outline of image simulation. (a) A 'testcard' specimen is defined as a set of fluorophore positions, in this case crossing lines of fluorophores at 16 nm separation (horizontal) and 23 nm (diagonal). A random subset of fluorophores (red) are set to be in the active (bright) photoswitching state. The optical point spread function of each fluorophore is integrated over a simulated CCD grid and realistic photon detections are assigned to each pixel (b), and then random camera noise is added to the image (c). A stack of such images are simulated independently, to provide data for testing localization algorithms.

2.2. Experimental methods

HeLa cells were grown in RPMI 1640 without phenol red (Gibco/Invitrogen), supplemented with 100 units ml^{-1} penicillin, 100 $\mu g\ ml^{-1}$ streptomycin, 1 mM L-glutamine, 10% foetal calf serum (FCS), and plated in LabTek II 8-well chambered coverglass (Nunc). After 12–24 h, the medium was replaced with medium without FCS and the cells were incubated with unlabelled Aβ_{1-42} (BachemGmbh, Weil am Rhein, Germany) for 1 h prior to fixing them using 3.7% paraformaldehyde (Sigma, Germany) in PBS for 10 min. The fixed cells were washed three times with PBS and permeabilized in PBS 0.5% v/v Triton X-100 (Sigma, Germany) for 10 min. After three washing steps with PBS, the cells were incubated with 5% BSA in PBS. In order to stain the unlabelled Aβ_{1-42} indirect immunochemistry was applied, i.e. cells were stained with a monoclonal anti-β Amyloid antibody (6E10) (Covance, Leeds, UK) and Alexa Fluor® 647 goat anti-mouse IgG antibody (Invitrogen, Paisley, UK), respectively, for 60 min. After each staining step three washing steps were performed using PBS, 0.1% v/v Tween 20 (Sigma, Germany).

For imaging, the specimens were immersed in a 'switching buffer' of phosphate-buffered saline (PBS), containing 0.5 mg ml^{-1} glucose oxidase (Sigma, Germany), 40 $\mu g\ ml^{-1}$ catalase (Roche), 10% w/v glucose and 100 mM β-mercaptoethylamine (MEA) at pH 7.4–8.5. The *d*STORM method was employed [4] using an Olympus IX-71 inverted microscope with an oil-immersion objective (PlanApo 60×, NA 1.45, Olympus), and total internal reflection fluorescence (TIRF) illumination. Laser illumination at 642 nm was applied at 1–10 kW cm^{-2} on the specimen. Fluorescence images were collected on a Andor iXon DV897 EMCCD camera. 20 000 frames of raw image data were captured with 10 ms exposure time.

2.3. Image analysis and reconstruction of the super-resolved image

Raw image stacks were analysed using a framewise 'segmentation and Gaussian fitting' algorithm designed for localization microscopy with sparse image data. Each raw image was segmented to find bright spots, by first of all averaging with a 3 × 3 top-hat convolution filter to suppress noise, and then identifying local maxima that are brighter than a user-defined threshold as candidates for localization. The fluorophore position of each candidate was determined by iterative Gaussian fitting. Corresponding localization parameters that were fitted simultaneously were retained for quality control: the number of photons of signal associated with each candidate, the fitted PSF width in both the *x*- and *y*-directions, and an estimate of the background noise level in the image. Candidates were rejected which exhibited too-imprecise a localization precision, based on Thompson's equation [18] for localization precision Δ when N photons are imaged with a PSF of variance s^2 on a camera with pixel width a and noise equal to b photons per pixel.

$$\Delta^2 = \frac{s^2 + a^2/12}{N} + \frac{8\pi s^4 b^2}{a^2 N^2}. \quad (1)$$

Accepted localizations for which the localization precision was better than a user-chosen value were visualized in terms of fluorophore density by rastering them as a 'histogram image' [7, 10]. The MATLAB routines developed for image simulation and processing are available from [20].

3. Image processing summary

The three general functions of localization microscopy software are: (a) localization, (b) quality control and (c) visualization, which are worth discussing in order. We should note that localization microscopy software tools can offer a choice of algorithms for each step, and it is important to pick one that works effectively for the data in hand.

Localization algorithms may be designated for spatially 'sparse' or 'dense' fluorescence images. Sparse algorithms perform fluorophore position inference based on the assumption that the raw data contain non-overlapping spots, so that bright spots can easily be found by 'segmentation' before applying an accurate fitting routine to determine the precise positions of these candidates. A common further assumption is that the frames of raw data are temporally independent, so that localizations can be identified in parallel for each frame without concern for artefacts that might be

introduced by fluorescence images which persist across many consecutive frames—this assumption can later be relaxed by using post-processing to identify and address any such issues. The properties of sparse algorithms are well established based on their history in particle tracking [21]. Techniques based on using a Gaussian fitting method to determine the centre position of a spot are found to be efficient and accurate when applied to sparse data, as well as being simple to implement, and these are probably the most popular sparse algorithms in current use [9, 10]. Because of their relative simplicity, sparse localization algorithms benefit from simple and robust metrics of quality. For example, the average Thompson precision of sparse localizations can be evaluated to estimate the resolution of the reconstructed super-resolution image [14]. The disadvantage of sparse algorithms is that regions of a specimen which actually exhibit overlapping fluorescence images can lead to spuriously high or low numbers of localizations, and thus to a reconstructed image that contains incorrect and misleading features.

Dense algorithms identify fluorophore positions based on raw image data that may contain spatially overlapping as well as sparse PSFs. This enables super-resolution images to be obtained from specimens with only a limited photoswitching ratio; and this also leads to better time resolved data, because fluorophore positions can be determined more rapidly [22]. There are several types of dense localization algorithm. DAOSTORM is based on an established method in astronomy, and iteratively fits multiple PSFs to regions of image data which appear to contain overlapping signals [11]. This method has the advantage of identifying separate parameters such as the number of photons of signal and the PSF width for each localization; however cross-talk between the inferred parameters of adjacent localizations poses a challenge to this evaluation. Compressed sensing can extract fluorophore co-ordinates from potentially overlapping image data, by applying a matrix inversion of a known forward problem—that is to say by first calculating the expected fluorescence image from each possible fluorophore position (with a chosen granularity) and determining the fluorophore positions that give rise to real signals in light of this complete prior knowledge [12]. This method uses well established signal processing methods, but is not well equipped to identify key quality control parameters such as the PSF width of each fluorophore image. The ‘Bayesian Localization Microscopy’ 3B-analysis optimizes a model of fluorophore density to fit the fluorescence measurements made in a whole series of images [13]. This method is computationally demanding, but aims to make use of the entire information content in a dense image stack, allowing for reconstructions using fewer frames of data and hence faster time resolution. The methods used by these dense algorithms are outlined in supplementary figure 1 (available at stacks.iop.org/JOpt/15/094012/mmedia).

One basic drawback of dense algorithms is that they are computationally slower: whereas sparse localization is typically possible at real-time frame rates, dense localization may slow down an experimental workflow. More problematically, since they are more complex and designed to process challenging data, their eventual misbehaviour at low signal to noise ratios may be hard to spot. Further, the potential cross-talk between the properties of localizations made using overlapping image data means that applying quality control criteria to these localizations is challenging. Finally, the best localization precision, and hence the best image resolution, tends to require sparse image data, and both sparse or dense algorithms can achieve equally high precision in this case [11, 12]. The advantage of dense algorithms is that they still produce reasonable precision with dense image data, which allows faster time resolution, down to at least 2 s [22]. However, if the aim of an experiment is to achieve the best possible resolution, then the experiment should be set up to measure sparse image data, in which case there is little loss from using a sparse localization algorithm, and some complexity can be avoided.

The purpose of a quality control algorithm is to reject spurious or imprecise localizations that arise from camera noise, fluorescence background, or weak fluorescence signals. This step is usually combined with visualization in a post-processing workflow that is separate from the time-consuming localization algorithm. Following sparse localization algorithms, typical quality control criteria are: candidate brightness, fitted PSF width (rejecting broad spots excludes out of focus signals and aggregates), or residual (rejecting candidates with a substantial square error between the signal and the fitted PSF). In practice, an effective method of quality control is to estimate the uncertainty of each localization using equation (1) [18], and exclude candidates less precise than a threshold value. This is a highly effective method of quality control in practice, since the localization precision is directly related to the resolution of the reconstructed image [14]. Hence this is recommended as a simple one-parameter method of quality control. Quality control of localizations obtained by dense localization algorithms may have to use more complex measures of quality, since separate precisions for each localization may not be determinable. Among the dense algorithms, DAOSTORM seems best able to separate information about each localization so that its precision can be estimated using equation (1), enabling a simple quality control method.

Visualization methods convert localized fluorophore positions into an image that represents the fluorophore density of the specimen. Baddeley proposed some optimized image reconstruction techniques [7], based on identifying the key visualization properties as: (a) linearity with specimen fluorophore density, (b) structure preservation, (c) no loss of resolution contained in the data, (d) communicating the achieved resolution to the viewer, (e) non-introduction of artefacts or implied resolution better than the real value, and (f) robustness (i.e. a minimum of adjustable parameters). The key challenge for an optimal visualization is therefore that the localizations are sufficiently smoothed that they do not imply a pointillist structure where there is none, and simultaneously that it does not smooth the data so much that real structures are blurred out and lost. Ideally, each localization should be smoothed by an amount that depends on its localization precision, as well as the local density

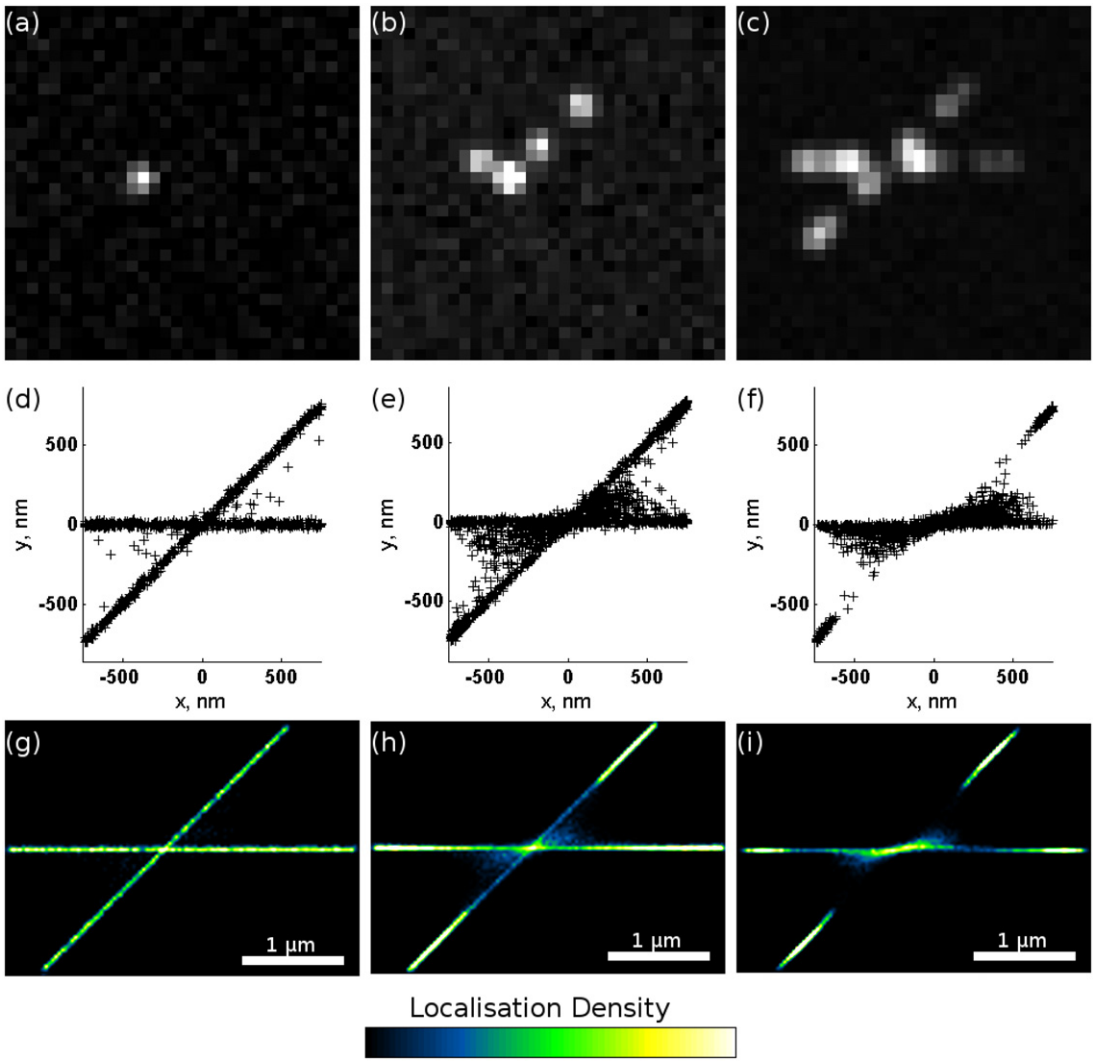

Figure 3. Effect of fluorescence density on the results of a sparse localization algorithm (simulated). (a)–(c) Image stacks were simulated from the testcard object in figure 2(a), with decreasing photoswitching ratios defined to give increasingly dense fluorescence (from left to right). Localizations (d)–(f) and the corresponding super-resolution images (g)–(i) show that sparse fluorescence signals support a faithful reconstruction of the specimen; however denser fluorescence leads first to mislocalizations (h) and then to complete loss of the true structure (i). Note that in case (i) the denser horizontal line of fluorophores dominates and obscures the slightly sparser diagonal line near the crossing point.

of observed localizations [14]. The 'Gaussian rendering' method is one good way to achieve this [7], as is its digital equivalent the 'jittered histogram' [8]. The simple 'histogram visualization' is often used in practice, and the fixed pixel size of the reconstructed image corresponds to a homogeneous degree of smoothing. Although not ideal for samples with variable fluorophore density, this visualization is good when the fluorescent parts of the specimen have a uniform labelling density.

4. Effects of dense fluorescence data

The quality of a super-resolution image in localization microscopy depends strongly on how the choices of localization algorithm, quality control parameters, and visualization method interact with each particular dataset obtained from a specimen. This is illustrated in figure 3 using simulated image data produced from a 'testcard' object, which in this case is a pair of crossing lines labelled with fluorophores. Image processing for figures 3 and 4 was performed with a sparse algorithm as outlined in 2.3. Localizations are both plotted directly and visualized as a fluorophore density histogram reconstruction. We applied a single-parameter method of quality control, by excluding localizations with a precision worse than 40 nm estimated using equation (1). With sparse image data, the reconstruction is faithful to the structure. Moderately dense fluorescence data lead to mislocalizations: overlapping point spread functions are misinterpreted as localizations between the true linear features. At high fluorescence density some area of the true specimen are completely lost from the reconstructed image, because the extensively overlapping images produce mislocalizations which are rejected by the quality control criteria (too-wide PSFs seem to correspond

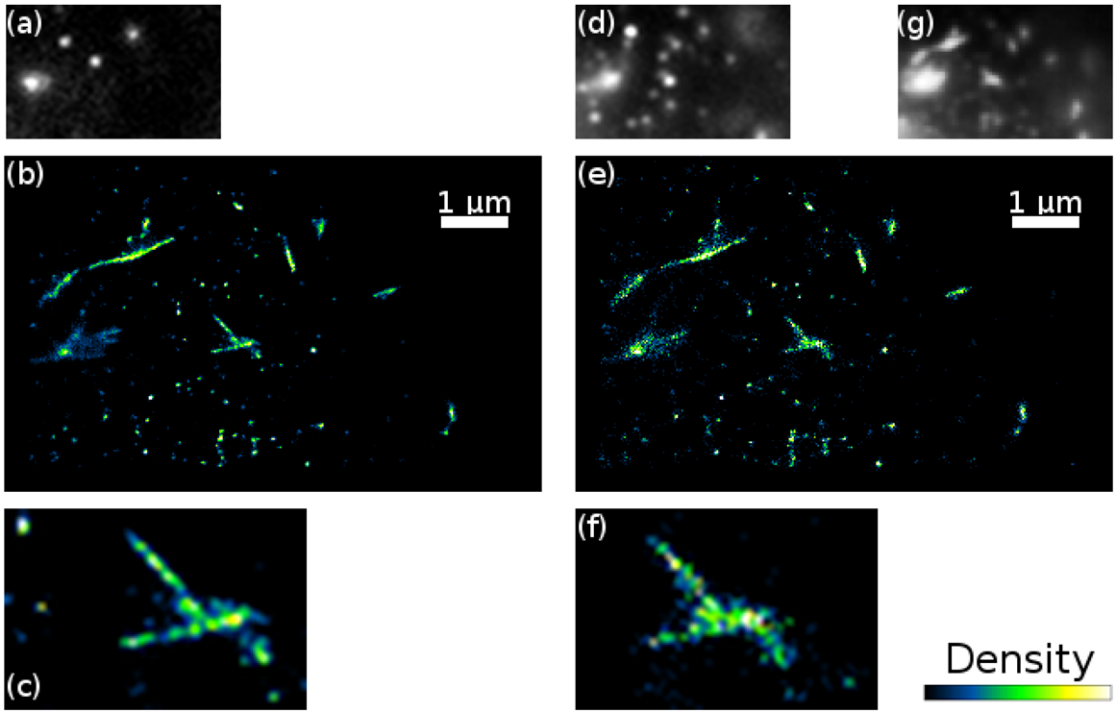

Figure 4. Effect of fluorescence density on experimental super-resolution images. Beta amyloid protein aggregates were imaged using the *d*STORM technique. The raw image data contained sparse fluorescence images (a), which were processed by a sparse localization algorithm to produce a robust super-resolution image revealing amyloid fibrils (b)–(c). Dense experimental measurements were generated by summing consecutive sets of 10 frames of raw image data, to emulate over-long exposure times. The dense fluorescence data (d) yielded a degraded super-resolution image (e) with mislocalization artefacts similar to those seen in simulation (f). In this case the mislocalization damage was not severe, and both reconstructions were better resolved than the conventional fluorescence image (g).

to poor localization precision). Figure 4 shows that similar damage occurs to super-resolution images of Beta amyloid fibrils when the observed fluorescence images are too dense. The artefacts seen here are similar to those seen in simulation: some mislocalization blurring is seen in the regions between crossing fibrils, and some fainter areas are blotted out by mislocalization with nearby dense areas. From the case of these amyloid fibrils, it is clear that potential artefacts of localization microscopy can be explored in advance by simulation, and this approach can be very helpful when interpreting super-resolution images.

5. Image processing software

The image processing and simulations for this paper were all performed using MATLAB routines that we have developed for localization microscopy, and which we make available under the name rainSTORM [20]. These routines can be used to perform the image processing element of localization microscopy, and includes the resolution analysis described in [14]. Additional scripts are included to perform: image simulation for testbenching and validation; batch processing of multiple files; fiducial marker tracking and drift correction; chromatic offset correction; and molecular trajectory imaging. Readers with some free time may like to refer to other localization microscopy softwares, which include: rapidSTORM [10], quickPALM [23], GraspJ [24], DAOSTORM [11], 3D-DAOSTORM [25], Compressed Sensing [12], 3B-Analysis [13], and Localizer [26].

6. Conclusions

This paper has reviewed the fundamental properties of image processing software in localization microscopy. The choice of sparse or dense localization algorithms has been discussed in detail, together with a study into the kind of artefacts seen when processing raw image data comprising denser fluorescence than the algorithm was designed to handle. Simulation is shown to provide a good qualitative guide to how the super-resolved image of particular structures may be degraded if the fluorescence data are denser than the ideal. A full set of MATLAB tools for localization microscopy, named rainSTORM, is provided as an aid for system development. In the near future, localization microscopy software seems likely to improve in several capabilities: (a) in simultaneously achieving dense and precise localization, (b) in offering simple quality control methods for handling dense localization data, and (c) visualization methods that are optimized for more sophisticated roles than reconstructing 2D fluorophore density—probably including 3D fluorophore density and molecular trajectory graphs.

Acknowledgments

This paper is based on work supported by the Engineering and Physical Sciences Research Council UK (EP/H018301/1), the Alzheimer's Research UK Trust (ARUK-EG2012A-1), the Wellcome Trust (089703/Z/09/Z), the Medical Research

Council (MR/K015850/1), and the Chemical and Biological Metrology Program of the UK's National Measurement Office. We thank Mark Deimund for assistance with developing the GUIs, Daniel Metcalf for experimental guidance and Professor Markus Sauer for inspiring discussions.

References

[1] Betzig E, Patterson G H, Sougrat R, Lindwasser O W, Olenych S, Bonifacino J S, Davidson M W, Lippincott-Schwartz J and Hess H F 2006 Imaging intracellular fluorescent proteins at nanometer resolution *Science* **313** 1642–5

[2] Huang B, Wang W Q, Bates M and Zhuang X 2008 Three-dimensional superresolution imaging by stochastic optical reconstruction microscopy *Science* **319** 810–3

[3] Folling J, Bossi M, Bock H, Medda R, Wurm C A, Hein B, Jakobs S, Eggeling C and Hell S W 2008 Fluorescence nanoscopy by ground-state depletion and single-molecule return *Nature Methods* **5** 943–5

[4] Heilemann M, Linde S, Schuttpelz M, Kasper R, Seefeldt B, Mukherjee A, Tinnefeld P and Sauer M 2008 Subdiffraction-resolution fluorescence imaging with conventional fluorescent probes *Angew. Chem. Int. Edn* **47** 6172–6

[5] Ferraro F *et al* 2013 The number of quanta of Von Willebrand factor determines the size and function of Weibel–Palade bodies *Nature Cell Biol.* submitted

[6] Kaminski G S, Linde S, Erdelyi M, Esbjorner E K, Klein T, Rees E, Bertoncini C W, Dobson C M, Sauer M and Kaminski C F 2011 *In situ* measurements of the formation and morphology of intracellular β-amyloid fibrils by super-resolution fluorescence imaging *J. Am. Chem. Soc.* **133** 12902–5

[7] Baddeley D, Cannell M B and Soeller C 2010 Visualisation of localization microscopy data *Microsc. Microanal.* **16** 64–72

[8] Krizek P, Raska I and Hagen G M 2011 Minimizing detection errors in single molecule localization microscopy *Opt. Express* **19** 3226–35

[9] Cheezum M K, Walker W F and Guilford W H 2001 Quantitative comparison of algorithms for tracking single fluorescent particles *Biophys. J.* **81** 2378–88

[10] Wolter S, Schuttpelz M, Tscherepanow M, Linde S, Heilemann M and Sauer M 2010 Real-time computation of subdiffraction-resolution fluorescence images *J. Microsc.* **237** 12–22

[11] Holden S J, Uphoff S and Kapanidis A N 2011 DAOSTORM: an algorithm for high-density super-resolution microscopy *Nature Methods* **4** 279–80

[12] Zhu L, Zhang W, Elnatan D and Bo Huang B 2012 *Nature Methods* **9** 721–3

[13] Cox S, Rosten E, Monypenny J, Jovanovic-Talisman T, Burnette D T, Lippincott-Schwartz J, Jones G E and Heintzmann R 2011 *Nature Methods* **9** 195–200

[14] Rees E J, Erdelyi M, Pinotsi D, Knight A, Metcalf D and Kaminski C F 2012 Blind assessment of localisation microscope image resolution *Opt. Nanoscopy* **1** 12

[15] Metcalf D J, Edwards R, Kumarswami N and Knight A E 2013 Test samples for optimizing STORM super-resolution microscopy *J. Vis. Exp.* at press

[16] Linde S, Löschberger A, Klein T, Heidbreder M, Wolter S, Heilemann M and Sauer M 2011 *Nature Protoc.* **6** 991–1009

[17] Laevsky G S and O'Connell C B 2013 Comparative and practical aspects of localization-based super-resolution imaging *Curr. Protoc. Cytometry* **63** 2.20.1–2.20.11

[18] Thompson R E, Larson D R and Webb W W 2002 Precise nanometer localization analysis for individual fluorescent probes *Biophys. J.* **82** 2775–83

[19] Dempsey G T, Vaughan J C, Chen K H, Bates M and Zhuang X 2011 Evaluation of fluorophores for optimal performance in localization-based super-resolution imaging *Nature Methods* **6** 1027–36

[20] http://laser.cheng.cam.ac.uk/wiki/index.php/Resources

[21] Crocker J C and Grier D G 1996 Methods of digital video microscopy for colloidal studies *J. Colloid Interface Sci.* **179** 298–310

[22] Shim S H, Xia C, Zhong G, Babcock H P, Vaughan J C, Huang B, Wang X, Xu C, Bi G Q and Zhuang X 2012 Super-resolution fluorescence imaging of organelles in live cells with photoswitchable membrane probes *Proc. Natl Acad. Sci.* **109** 13978–83

[23] Henriques R, Lelek M, Fornasiero E F, Valtorta F, Zimmer C and Mhlanga M M 2010 QuickPALM: 3D real-time photoactivation nanoscopy image processing in ImageJ *Nature Methods* **7** 339–40

[24] Brede N and Lakadamyali M 2012 GraspJ: an open source, real-time analysis package for super-resolution imaging *Opt. Nanoscopy* **1** 11

[25] Babcock H, Sigal Y M and Zhuang X 2012 A high-density 3D localization algorithm for stochastic optical reconstruction microscopy *Opt. Nanoscopy* **1** 6

[26] Dedecker P, Duwe S, Neely R K and Zhang J 2012 Localizer: fast, accurate, open-source, and modular software package for superresolution microscopy *J. Biomed. Opt.* **17** 126008